Corresponding State Behaviour of Vapour- Liquid Phase Equilibria of Bulk and Confined Alkanes

A Dissertation

Submitted in the partial fulfilment of the requirements for the award of degree

of

Masters of Sciences

In

Chemistry

Submitted By

Anjali

(Roll No.301502003)

Under the Supervision of

Dr. Sudhir K Singh

(Assistant Professor)

Department of Chemical Engineering

School of Chemistry and Biochemistry

Thapar University, Patiala-147004

July 2017

CERTIFICATE

This is to certify that the dissertation entitled "**Corresponding State Behaviour of Vapour-Liquid Phase Equilibria of Bulk and Confined Alkanes**" being submitted by Ms.Anjali in partial fulfilment of the requirements for the award of degree of Master of Science in Chemistry and being submitted to the School of Chemistry and Biochemistry, Thapar University, Patiala, is a bonafide work carried by her under our supervision. The work has reached the standard necessary for submission. The contents of this dissertation have not been submitted for the award of any other degree or diploma.

Sudhir Kr. Singh

Dr. Sudhir K.Singh
Assistant Professor
Department of Chemical Engineering
Thapar University, Patiala -147004

CANDIDATE'S DECLARATION

I hereby declare that the work being presented in the dissertation entitled "**Corresponding State Behaviour of Vapour- Liquid Phase Equilibria of Bulk and Confined Alkanes**" in partial fulfilment of the requirements for the award of degree of Masters of Science in Chemistry and being submitted to School of Chemistry and Biochemistry, Thapar University, Patiala, is my own work during the period of January to July 2017, under the supervision of **Dr. Sudhir K Singh**. I have not submitted embodied in this dissertation for the award of any other degree.

Anjali

Patiala **Anjali**

Date: 9 August, 2017

This is certify that the above statement made by the candidate is correct and true to the best of our knowledge.

Sudhir Kr. Singh.

Dr Sudhir K Singh
Assistant Professor
School of Chemistry & Biochemistry
Thapar University, Patiala-147004

ACKNOWLEDGEMENT

First of all, I owe my gratitude to the Head of the Department, **Dr. Amjad Ali** for providing me the opportunity in the form of this dissertation to develop my interest in research.

In the same spirit, I would like to thank my Supervisor, **Dr. Sudhir K Singh** for his constructive guidance and constant support during the project. The work presented here could not have been accomplished without their patience and ever willingness to teach. They have taught me to concise and correct in my approach from the formulation of ideas to the presentation of the results.

Special thanks to all the **Teaching Faculty** of the department for their cooperation and guidance.

I am grateful to **Thapar University & School of chemistry and biochemistry** for providing financial support and all necessary infrastructure and laboratory facilities to carry out the experimental work.

Words fail me to express my thanks to my family and friends who have always supported me and have been a source of strength and inspiration to me during the entire period of the work.

All the thanks are, however, only fraction of what is due to almighty for granting me an opportunity and strength to successfully accomplish this project.

Date: 9 August, 2017

Anjali

Anjali

ABSTRACT

In this work, we have investigated the corresponding state behaviour of vapour-liquid phase equilibria of bulk and confined alkanes using grand-canonical transition-matrix Monte carlo simulation and histogram reweighting method. In this work, Buckingham exponential-6 potential model is used to describe the interaction between alkane's molecules and Steele potential is used for the interaction between confining surface and alkane molecules. In this investigation methane, n-butane and n-octane are subjected under graphite and mica slit pores of varying slit width. In case of methane, slit width varied from $40A^0$ to $5.4A^0$, n- butane from $40A^0$ to $6A^0$ and for n-octane $50A^0$ to $10A^{0.}$ In these investigations deviations from corresponding state behaviour in vapour-liquid phase equilibria is observed with larger pore widths, irrespective of type of fluid under consideration. On the other hand, with smaller pore width insignificant deviations from corresponding state behaviour in vapour-liquid phase equilibria is observed. We have also compared the saturation vapour pressure in confinement with respect to bulk, in a corresponding state plot. Saturation vapour pressure under either type of confinement (graphite & mica) show positive deviation (with larger pore width) and negative deviation (with smaller pore width) with respect to the corresponding bulk value at a given reduced temperature.

LIST OF FIGURES

LIST OF CONTENTS

CHAPTER-4

CHAPTER-5

CHAPTER-6

CHAPTER-1

1. INTRODUCTION

1.1 Vapour-liquid phase equilibrium

A fixed situation where no alterations occur in the macroscopic properties of a system with time is known as Equilibrium state. So, Vapour-liquid Equilibrium is a state in which a liquid and its vapour are in equilibrium with each other, means where the amount of evaporation is the same to the amount of condensation on a molecular level such that there is no overall vapour liquid inter-conversion. The behaviour of a liquid-vapour system with Temperature-Volume at constant pressure is shown below in Figure1.1. The plots obtained are called isobars.

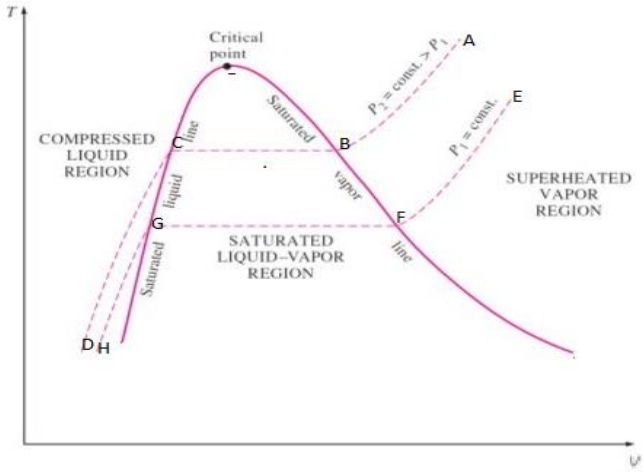

Figure 1.1 T-V diagram for two phase system showing isobars.

At constant pressure, at point A, gaseous state exists. As the temperature is decreased, the volume of the gas decreases along the curve AB. At the point B, liquefaction of the gas starts. Hence volume decreases rapidly along BC because liquid has much less volume than the gas. At the point C, liquefaction is complete. Now the decrease in temperature has very little effect upon volume because liquids are very little compressible. Hence a steep curve CD is obtained.

In the area where both liquid and vapour occur, there are two bounding situations. When the last drop of vapour condenses, the state becomes saturated liquid. However, saturated vapour is the state where the last drop of liquid evaporates.

1.2 Basic of corresponding state

This theorem of corresponding permits that for all fluids, the value of compressibility factor is same when related at the same reduced temperature and reduced pressure. The value of P, V and T in reduced form is:

The reduced volume is the ratio of the molar volume to the critical molar volume:

$$V_r = \frac{V}{V_C} \qquad \text{(A)}$$

The reduced pressure is the ratio of the pressure to the critical pressure:

$$P_r = \frac{P}{P_C} \qquad \text{(B)}$$

The reduced temperature is the ratio of the temperature to the critical temperature:

$$T_r = \frac{T}{T_C} \qquad \text{(C)}$$

1.3 Confined Fluids (Alkane)

Constrained to area or volume is called confinement. So, in a macroscopic world, fluids confined by surrounding surfaces of any form or shape that are visible by the normal human eye are defined as confined fluids. Fluids in macroscopic confinement do not show significant changes in their thermodynamic properties, since the number of molecules away from the surrounding surfaces is astronomically higher than the number of molecules in close proximity of the confining surfaces. Whereas, in microscopic confinement, however, the number of molecules away from the close proximity of the surface is not as high as is the case with macroscopic confinement. Hence, under the same thermodynamic conditions various thermodynamic properties at microscopic confinement may not remain the same as the bulk (macroscopic) values.

1.4 Basic Science behind Confinement

Collision of molecules occurs with each other or with the walls of pore in a porous solid. When the size of stoma is quite larger, the amount of interactions between the molecules and the walls of stoma is insignificant whereas the amount of interactions of molecules having

with each another is significant. However, this statement is not accurate as the stoma size gets reduced [1]. In close-fitting reservoirs, stoma sizes get similar with the size of the particles of fluid trying to run over them [2]. Figure 1.2 illustrates this effect schematically. The red molecule shows that it is interacting with the pore wall at a certain time. As we know a nano pore can grip less molecules with respect to macro-pores, so the vander walls interaction of molecules with each other and among the molecules and the pore wall increases. Such a condition is termed to be 'confinement of fluid. Because the free pathway obtainable to the molecules is circumscribed by the geometry of the void space of pore. Therefore we can conclude that this effect of confinement is observable, when the fraction of pore size to molecule size is less than 20 i.e., nano pore

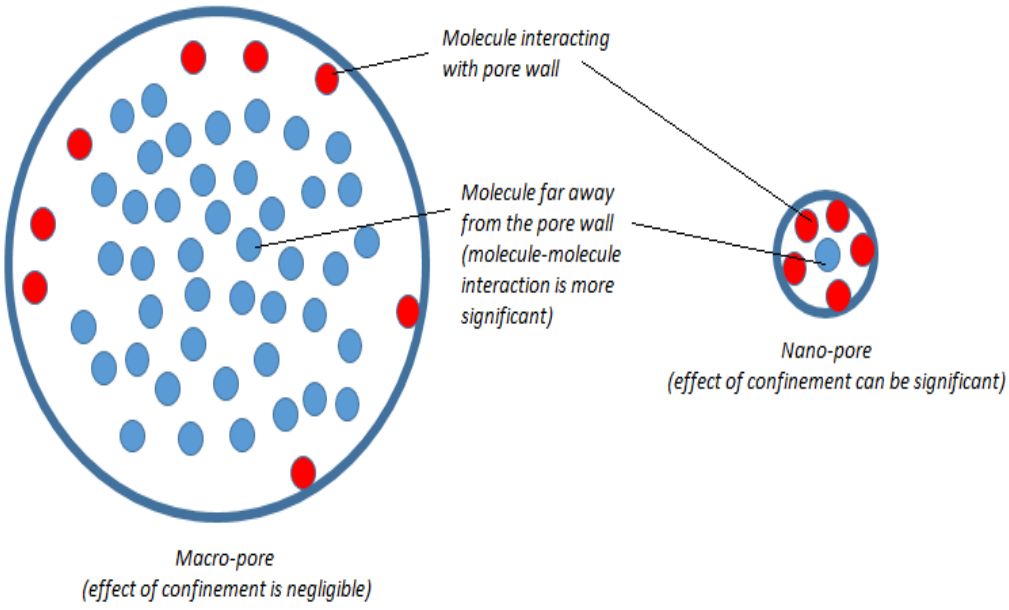

Figure 1.2 Effect of confinement in macro and nano pore.

In the surface layer molecules' properties is affected by increasing interactions between pore wall and fluid which give results to modification in dynamics of molecules in the surface layer sticking to pore wall (Chandra, 2014) as shown in Figure 1.2 in red colour. Overall, understanding the position of molecules in confinement is very complicated and not fully understood through theoretically and experimentally both.

1.5 Necessity of Confined Alkanes

Commonly, alkanes are used in several trades or production. They are found in polymers, oils, fuels, surfactants as well as in numerous organic molecules such as lipids. Under nano

confinements the behaviour of alkanes is very interesting from fundamental and practical view. For example: in chemical reactions micro and mesoporous materials are broadly used for pollution control, purification as well as catalyst and catalyst supports. The fundamental understanding of the several thermo physical and interfacial phenomena, in the presence of surfaces, is necessary for many industrial and geophysical operations in addition with finite size effects, changing dimension and competition between fluid-fluid and surface-fluid interactions. While, the practical view of fluids in confinement have numerous uses, for example in catalysis, oil recovery, colloidal stabilizations, membrane separation, nano material fabrication, storage of natural gas and hydrogen in nano porous materials. In overall, fluids show positive deviation from bulk thermo physical and structural properties in any kind of confinement inside pores of nanometres size. In any real system, an additional free energy influences because of the interfaces either with the walls of container or with different phases of the material under consideration. This free energy shows a vital role in nano confined systems and affects the state of the substance. Therefore in such system due to the interface between fluid-wall and fluid-fluid forces can lead to interesting surface-driven phase deviations and a number of other thermo physical and interfacial phenomena. Hence, the studies on confined fluids explain the change in thermo physical properties.

Such confinement effects on various thermo physical and interfacial properties, can be easily understand by molecular simulation [3]. To learn the adsorption properties of normal and branched alkanes in several porous materials such as zeolites, molecular simulations have been applied. Similarly, by using gauge-cell Monte Carlo simulation was applied to study the adsorption and separation properties of mixtures of *n*-alkanes in a carbon nanotube. In such nano tube confinement of *n*ormal alkanes decreases its critical temperature and increases its critical density was observed by the investigators. Recently, a methodology was used for metal-organic frameworks to study the adsorption characteristics of novel metal-organic materials for methane and hydrogen storage applications using molecular simulation. In some recent work single-component adsorption of methane, ethane, and some other higher *n*-alkanes along with its adsorption isotherms and density and orientation profiles was investigated in carbon slit pores using Monte Carlo simulations. These investigations indicate that there is an intense influence of the slit surfaces on the vapour-liquid thermodynamic properties.

1.6. Objectives of Current Work

The objective of current work is to study the corresponding state behaviour of vapour- liquid phase equilibrium of bulk and confined alkanes using molecular simulation techniques. The principle of corresponding states has a firm foundation in statistical mechanics. Precisely, we looked at the vapour-liquid phase transitions, critical properties and corresponding states behaviour. We address, for the first time in detail, the effect of surface chemistry and degree of confinement on the corresponding state behaviour of confined alkanes. Our investigations also reveal the effect of pore geometry and surface chemistry on the crossover behaviour from 3D (bulk-like) to 2D – like behaviour.

Such studies can be helpful in understanding and controlling the fluid film behaviour confined between solid surfaces of few molecular diameters, for example, in lubrications applications. When intermolecular interactions can be described by a functional form incorporating two parameters (usually a length and an energy scale), all intensive properties can be written in non-dimensional form as functions of (T^*, P^*) or (T^*, V^*). Where, T^*, P^*, and V^* are non−dimensional temperature, pressure and volume respectively. The principal of corresponding states often invoked to predict the thermo physical properties for a given compound once it's critical constants are known [4,5].

In this work, by performing rigorous computer experiments (computer simulations) using, (GC-TMMC) grand canonical transition matrix Monte Carlo simulation technique [6]. We investigated and compared the corresponding states vapour – liquid phase behaviour of bulk n-alkanes and the confinement of n-alkanes in mica and graphite slit pore of varying slit widths.

CHAPTER-2

REVIEW OF LITERATURE

The vapour-liquid equilibrium of the square-well model fluid of variable range was studied in 1996, which exhibits deviations from corresponding states behaviour [7].The principle of corresponding states works best for small, non-polar compounds with approximately spherical shape [8]. The principal of corresponding states was established in classical statistical mechanics, it has been clear that a conformal change in the intermolecular potential leads to a simple re-scaling of the thermodynamic properties of a bulk fluid [9]. Non-spherical and electrostatic forces also introduce deviations from corresponding states behaviour, and have been studied by some investigators [10-13]. The simplest three-parameter fluid model is the square-well fluid. Interest in the square-well fluid has produced a great deal of theoretical and numerical calculations. It has been observed that most classes of bulk real fluids do not follow the principal of corresponding states. Some studies also reflect the influence of non-conformal changes in potential on the vapour–liquid equilibrium of the bulk fluid. For example, square–well fluids (three parameter fluid model) with different ranges do not follow the corresponding state principle. In above study analysis was focused on the dependence on the square-well range, which exhibits deviations from corresponding-states behaviour. In a recent work [14] Mie and Yukawa model fluids have shown remarkably collapsing corresponding state behaviour yielding the same master curve for studied attraction ranges. However, for the square-well model fluids, two different master curves of corresponding state behaviour is observed. This behaviour of square-well fluid is attributed to the change in the shape of the coexistence curve from nearly cubic shape to nearly quadratic shape, which in turn reflected to their different effective critical exponents. This change of effective critical exponents impedes producing a single master curve.

Although, there are many theoretical and simulation studies on bulk [15-18] and confined [3, 19-22] vapour-liquid-phase equilibria of model fluids, however, detailed studies on corresponding-states behaviour of the vapour-liquid phase equilibria of fluids are scarce.

In 2002, Coupled-decoupled configurational -bias Monte Carlo simulations in the Gibbs ensemble were carried out to determine the vapour-liquid coexistence curve and critical properties for n-triacontane and 2,6,10,15,19,23-hexamethyltetra-cosane.

Vanderlick et al. developed an exact statistical mechanical solution, which can be used to investigate the thermodynamic properties of fluids confined to micropores [23] .Zarragoicoechea and Kuz (2004) documented the difference in phase behaviour of confined fluids when compared to bulk fluids. They showed that to properly account for the behaviour of confined fluids, the critical properties of the components must be altered as a function of the ratio of the molecule size to the pore size [24]. In another study, Zhang and Wang (2006) showed the critical point shift due to confinement and they investigated the impact of the change in wall fluid interaction [25]. Singh et al. (2007) has led the Configurational-bias grand canonical transition-matrix Monte Carlo simulations to research different thermophysical properties, such as phase coexistence, critical properties, density and orientational profiles of fluid and vapour phases and vapour fluid surface tension of methane, ethane, propane, n-butane and n-octane in bulk and slit pores of graphite and mica surfaces.
When phase envelope is crossed in gas condensate systems, there is a large gas oil volume split in the nano, meso and macro pores [26]. This is presumed to be responsible for economical production of liquids in such systems. Simulations and experimental data reveal that critical properties of many compounds change as pore size decreases [27]. It was illustrated by Kuz (2002) [28] that in order to properly account for the behaviour in confined fluids, the critical properties of components should be altered as a function of the ratio of molecule to pore size. They developed a correlation for the deviation of critical temperature and pressure from vander waal equation of state (EOS) by studying confined fluids in square cross section pores. Though they neglected the interaction between the fluid molecules and the wall, they did find good agreement between the predicted capillary condensation and critical temperature and experimental data.

In 2007, Hamada [29] used grand canonical Monte Carlo numerical simulations to study thermodynamic properties of confined Lennard-Jones (LJ) particles in slit and cylindrical pore systems and indicated changes in fluid phase behaviour as a function of pore radius. Singh (2009) investigated the behaviour of methane (C1), n-butane (C4) and n-octane (C8) inside nanoscale slits with widths between 0.8 to 5 nm using grand canonical Monte Carlo simulations and found out that while critical temperature decreased with reduction in pore

radius, the critical pressures of n-butane and n-octane first increased and subsequently decreased. They also found that the critical property shift is dependent on pore surface types and hence differed for mica and graphite. This work is of importance as shale rocks are characterized by organic and inorganic pore systems, both of which vary in mineral composition and thus will cause different intensities of pore wall and molecules' interaction [30].

In 2014 Teklu [31] extended the work of Singh to Bakken fluid sample and founded that shifts in critical properties led to the suppression of Bakken fluid phase envelope. Alharthy also used the correlations developed by Singh (2009) to investigate the impact of confinement on various variations of Eagle ford composition. They found that shift in critical properties led to an increase in condensate production and this increase was a function of both pore size, as well as fluid composition. In this work we have investigated and compared the corresponding state behaviour of normal alkanes, confined in mica and graphite slit pores of different slit widths.

In the Chapter 3, we briefly describe the molecular simulation Methodology and techniques used to estimate the corresponding states behaviour of bulk and confined n-alkanes.

CHAPTER-3

3.1. METHODOLOGY

3.1.1. Introduction to Monte Carlo Simulations

Monte Carlo simulations may be defined as a set of methods in which the individual position and conformation of every molecule in the system is explicitly accounted. In compensation, molecular simulation can consider much larger systems, and this often makes it possible to derive observable macroscopic properties (i.e. that can be compared with measured experimental quantities) using microscopic information provided by the well-established framework of statistical thermodynamics. Monte Carlo methods are most suited for calculation by computer. In molecular simulations, Monte Carlo is almost always used to refer to methods that use a technique called importance sampling. Importance sampling methods are able to generate states of low energy, as this enables properties to be calculated accurately.

The Metropolis algorithm generates a Markov chain [32] of states which satisfies the following two conditions:

a) The outcome of the each trial depends upon the preceding trial and not upon any previous trials.
b) Each trial belongs to a finite set of possible outcomes.

Monte Carlo simulation involves the repeated application of an elementary procedure as follows:

1. A trial configuration is generated by perturbing the original configuration of particles e.g. a randomly selected atom is moved by small amount from its present position.
2. The ratio of probabilities, as per detailed balance [33] for the trial and original configurations is computed, and from this quantity a decision is made whether to accept or reject the trial.
3. If the trial is accepted, the new configuration is taken as the next state in the Markov chain; otherwise the original configuration is taken as the next state in chain.
4. Average properties of interest are collected over many independent configurations generated using the above steps.

The schematic of the above elementary procedure can be represented as shown in Figure 3.1.

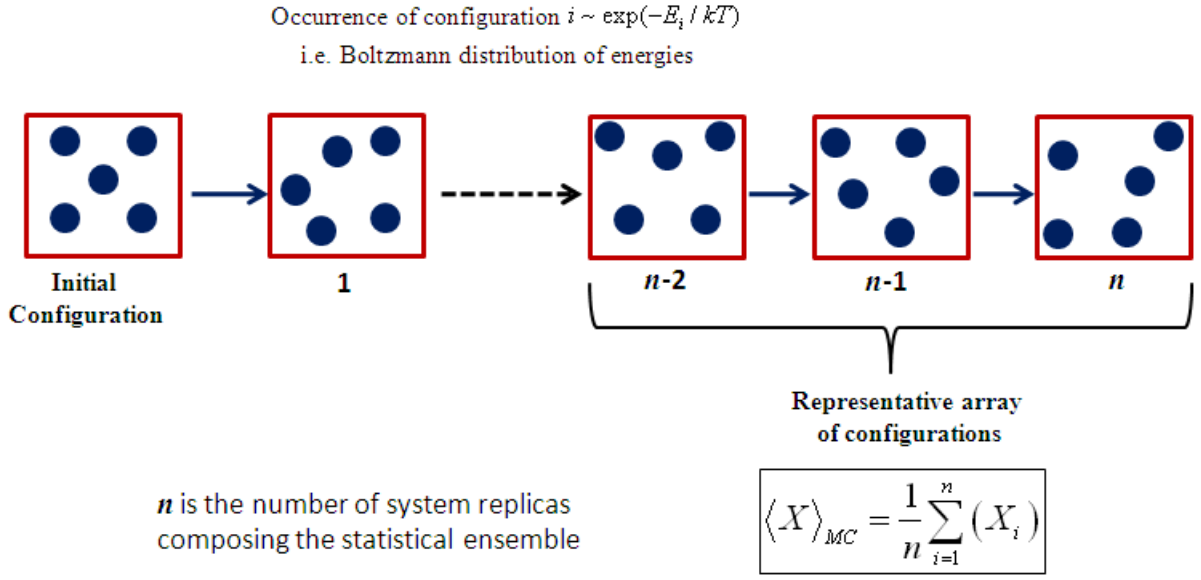

Figure 3.1 Schematic of a Monte Carlo Simulation in the perspective of the canonical ensemble. Symbol X represents the average property such as E, V, P i.e. average energy, volume and pressure respectively.

Depending upon the ensemble used for the simulation process in general, Monte Carlo simulation is categorized into five classes:

1 **NVE-MC:-** It is micro canonical ensemble where number of particles, volume and energy are kept constant during simulation.

2 **NVT-MC:-** This canonical ensemble in which number of particles, volume and temperature are kept constant during the simulation.

3 **NPT-MC:-** It is isothermal–isobaric ensemble where number of particles, pressure and temperature are kept constant during the simulation.

4 **GE-MC:-** A particular case of Monte Carlo simulation in which interface energy is not accounted for. In this Gibbs ensemble, both temperature and the total number of particles are fixed, and we can impose either i.e. the sum of phase volumes or pressure.

5 **μVT-MC:-**This is also GCMC, grand canonical ensemble, where chemical potential (μ), volume and temperature are kept constant, while number of particles fluctuates during the simulation. This ensemble is most convenient statistical ensemble to simulate e.g.

adsorption isotherms, interfacial properties, either of pure compounds or multi-component systems and gives a means to compare the experimental results explicitly. The basic concept in GCMC simulation is to exchange the particles from a reservoir to sub system and vice versa keeping the chemical potential, μ, constant. We assume that the molecules in the two sub volumes are actually identical particles. The only difference is that when they are in the volume *V*, they interact and when they are in the volume $V_0 - V$, they do not. The key feature about the GCMC method is that the number of particles may change during the simulation.

There are three basic moves in a GCMC simulation:

I) **Displacement Trial Move**:-A particle is displaced in the simulation box, using the usual Metropolis method.

II) **Deletion Trial Move**: - A particle is removed from the simulation box.

III) **Insertion Move Trial**: - A particle is added at a random position in the simulation box. These basic moves are schematically shown in the Figure 3.2. Moreover, for chain molecules two more moves, rotation and regrowth of particle are incorporated along with the above mentioned basic moves.

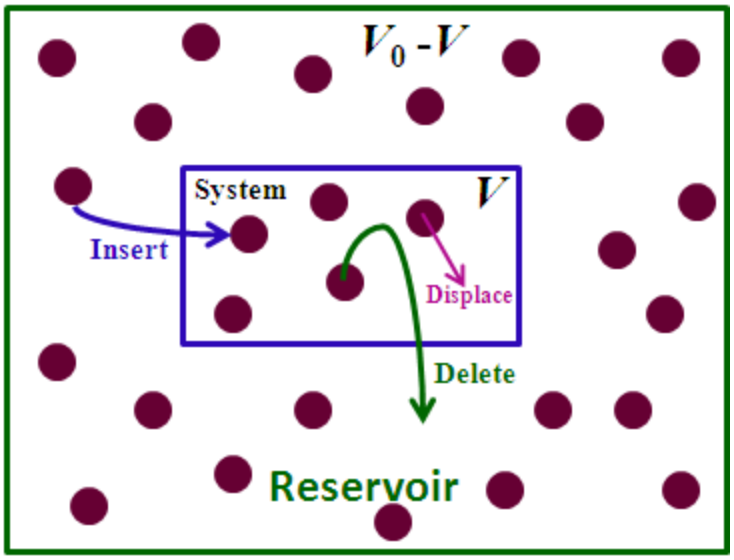

Figure 3.2 A schematic of GCMC basic moves during simulation.

In the current work, we have used GCMC technique to study the phase transition and interfacial property of confined fluid. More specifically, we have used the technique known

as Grand canonical transition matrix Monte Carlo (GC-TMMC) along with a multicanonical sampling scheme [34] to explore the configuration space more efficiently.

Further, histogram reweighting [35] technique is employed to locate the coexisting phases. Moreover, for chain molecules united atom approach [36] is used, where we neglect the hydrogen atoms; however, the influence of hydrogen atoms is considered through the parameterisation of potential parameters. Additionally, for chain molecules a configurational-bias technique [37] is incorporated within the GC-TMMC framework.

3. 2 Simulation Methods

3.2.1. Potential Model

An assembled atom approach [38] (An assembled-atom is a particle that incorporates a group of atoms but can approximately represent the molecular mechanical properties of the group on a scale of size that is larger than atomic scale. It is also called pseudo-atom.) is utilized to demonstratethe n-alkane molecules. With the modified Buckinghim exponential intermolecular potential of Errington and Panagiotopoulos [39] non-bonded site-site interactions are described which is represented as:-

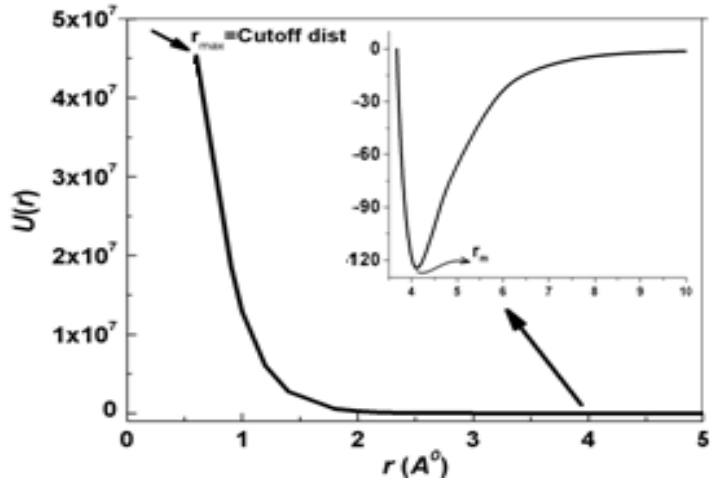

Figure 3.3 Fluid-fluid potential energy (U_r) versus distance for the Buckingham exponential potential.

The Buckingham potential describes the interactions of two neutral particles using following mathematical model. Two neutral molecules feel both attractive and repulsive forces based

on their relative proximity and polarizability.

$$U(r) = \left\{ \frac{\varepsilon}{1 - 6/\alpha} \left[\frac{6}{\alpha} \exp\left(\alpha \left[1 - \frac{r}{r_m} \right] \right) - \left(\frac{r_m}{r} \right)^6 \right] \right\} \quad \text{for} \quad r > r_{\max},$$
$$= \infty \quad \text{for} \quad r < r_{\max}, \tag{1}$$

Where ε, r_m and α are flexible parameters. The variable r_m is the radial separation at which $U(r)$ achieves a minimum and the cut off separation $r_{\max}$ represents the smallest radial separation for which $d(U(r))/d(r) = 0$. The radial separation for which $U(r) = 0$ is signified by σ. The parameters ε, σ and α are 129.63 K, 3.679 Å, and 16 respectively, for the methyl group (-CH_3) 73.5 K, 4.00 Å, and 22 respectively, for the methylene group (-CH_2-), and 160.3 K, 3.73 Å and 15 respectively, for CH_4.

The following joining rules are utilised to determine the cross parameters:

$$\sigma_{ij} = \frac{1}{2}\left(\sigma_i + \sigma_j\right),$$
$$\varepsilon_{ij} = \left(\varepsilon_i \cdot \varepsilon_j\right)^{1/2},$$
$$\alpha_{ij} = \left(\alpha_i \cdot \alpha_j\right)^{1/2}. \tag{2}$$

The bond lengths CH_3–CH_3, CH_3–CH_2, and CH_2–CH_2 are 1.839 Å, 1.687 Å, and 1.535 Å, separate. Bending angles of bond are generated according to the bending potential [40].

$$u_{bend}(\theta) = \frac{K_\theta}{2}(\theta - \theta_{eq})^2, \tag{3}$$

Where K_θ = 62500 K/rad^2 and θ_{eq} = 114°. Torsion angles are generated according to the following potential

$$u_{tor}(\phi) = V_0 + \frac{V_1}{2}(1 + \cos\phi) + \frac{V_2}{2}(1 - \cos 2\phi) + \frac{V_3}{2}(1 + \cos 3\phi), \tag{4}$$

Where V_0 = 0, V_1 = 355.03 K, V_2 = -68.19 K, and V_3 = 791.32 K.

In this work, pore is of slit geometry with smooth and structure less surfaces. Wall-liquid interaction is depicted by the 9-3 Steele potential [41].

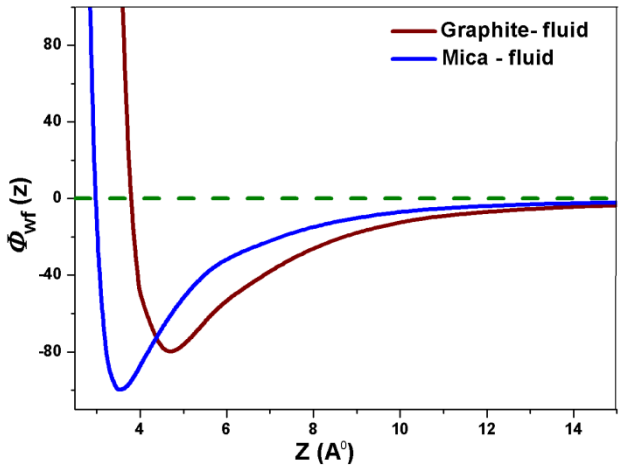

Figure 3.4 Wall-fluid potential energy versus distance from the wall for the Steele potential

$$\phi_{wf}(z) = \frac{2}{3}\pi\rho_w\varepsilon_{wf}\sigma_{wf}^3\left\{\frac{2}{15}\left(\frac{\sigma_{wf}}{z}\right)^9 - \left(\frac{\sigma_{wf}}{z}\right)^3\right\}, \qquad (5)$$

Where z is the separation of the liquid particle from the wall and ρ_w, ε_{wf} and σ_{wf} are the parameters of the Steele potential. In Eq. (5), $\sigma_{wf} = (\sigma_w + \sigma_{ii})/2$ where σ_w represents the "diameter" of a wall atom and σ_{ii} refers to the molecular diameter of corresponding CH_2-CH_2 or CH_3-CH_3- interactions. Potential parameters, ρ_w, ε_{wf} and σ_w for graphite and mica surfaces are 0.033 Å $^{-3}$, 84 K, 3.92 Å, and 0.097 Å $^{-3}$, 100 K, 2.22 Å, respectively whereas for methane σ_{wf} for graphite and mica surfaces are 3.7995 Å and 2.9805 Å respectively. [42].

3.2.2. Simulation Details

In this work, we have utilised configurational-bias grand canonical transition-matrix Monte Carlo, simulation scheme to explore configuration space more efficiently. Configurational-bias Monte Carlo technique is incorporated within the grand canonical transition-matrix Monte Carlo (GC-TMMC) framework along with multicanonical sampling scheme. In this approach, Monte Carlo simulations are conducted in a standard grand canonical ensemble where the volume (V), chemical potential (μ) and temperature (T) are held constant and the particle number N (density) and energy (U) fluctuates. During a simulation, attempted transitions between states of different densities are monitored. At regular intervals during a simulation this information is used to obtain an estimate of the density probability distribution, which is subsequently used to bias the sampling to low probability densities. Over time, all densities of interest are sampled adequately. The result is an efficient self-adaptive method for determining the density probability distribution over a specified range of densities (typically a range that corresponds to the densities of two potentially coexisting phases). Once a probability distribution has been collected at a given value of chemical potential (μ_0), histogram reweightingis used to shift the probability distribution to other values of the chemical potential using the following relation:

$$\ln \prod(N,\mu) = \ln \prod(N,\mu_0) + \beta(\mu - \mu_0) N \qquad (6)$$

To determine the coexistence chemical potential, we apply the above relation to estimate the chemical potential that produces a coexistence probability distribution. In above relation μ_o indicates the input chemical potential and μ represent the coexistence chemical potential. Phase coexistence is located by identifying the chemical potential value, μ, for which areas under the liquid and vapour domain of the probability distribution are equal. This is illustrated with Figure 3.5.

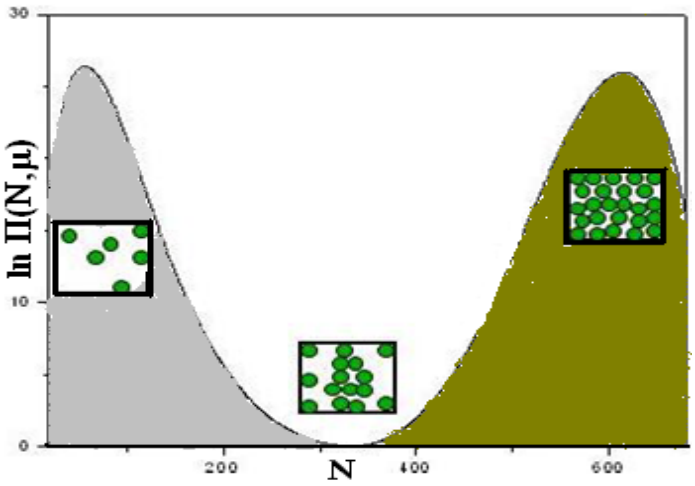

Figure 3.5 A schematic of coexistence probability distribution. The three boxes shown are the representative of the vapour–like (first peak), liquid–like (second peak) and intermediate/interface (minima) states.

Saturated densities are related to the first moment of the vapour and liquid peaks of the co-existence probability distribution, $\Pi_c(N)$. To calculate the saturation pressure we use the following expression

$$\beta PV = \ln\left(\sum \prod_C(N) / \prod_C(O)\right) - \ln(2) \qquad (7)$$

In addition to the calculation of saturation pressure, densities, and energies, GC-TMMC simulation can also yield the interfacial free energy for a finite system size with a cell length L, βF_L, which is determined from the maximum likelihood in the liquid $\prod^{l}_{\max}$ and vapour regions $\prod^{v}_{\max}$ and minimum likelihood in the interface region $\prod_{\min}$:

$$\beta F_L = \frac{1}{2}\left(\ln \prod^{l}_{\max} + \ln \prod^{v}_{\max}\right) - \ln \prod_{\min}. \qquad (8)$$

In this work, we have estimated the vapour-liquid critical parameter by fitting the coexistence densities to the law of rectilinear diameterand the scaling law for the density.

$$\left(\rho_l - \rho_v\right) = B\left(1 - \frac{T}{T_c}\right)^{\beta} \tag{9}$$

$$\left(\rho_l + \rho_v\right)/2 = \rho_c + A\left(1 - \frac{T}{T_c}\right) \tag{10}$$

Where, $\rho_l, \rho_v, \rho_c, T_c$, β are liquid phase density, vapour phase density, critical density, critical temperature, and critical exponent respectively.

Critical pressure, P_c, is calculated using the least square fitting of the following expression:

$$\ln P_c = A - \frac{B}{T_c} \tag{11}$$

Where, *A* and *B* are constants.

To perform the simulations in an efficient manner we take advantage of the fact that the TMMC algorithm enables one to fill the overall collection matrix through a series of independent simulations, each restricted to a limited range of microstates. In our simulations, the MC move distribution for evaluating phase coexistence properties is as follows: 15% particle displacement, 50% particle insertion/deletion, 15% particle rotation, and 20% particle regrowth.

CHAPTER-4

RESULTS AND DISCUSSION

4.1. Test of model with the experimental value

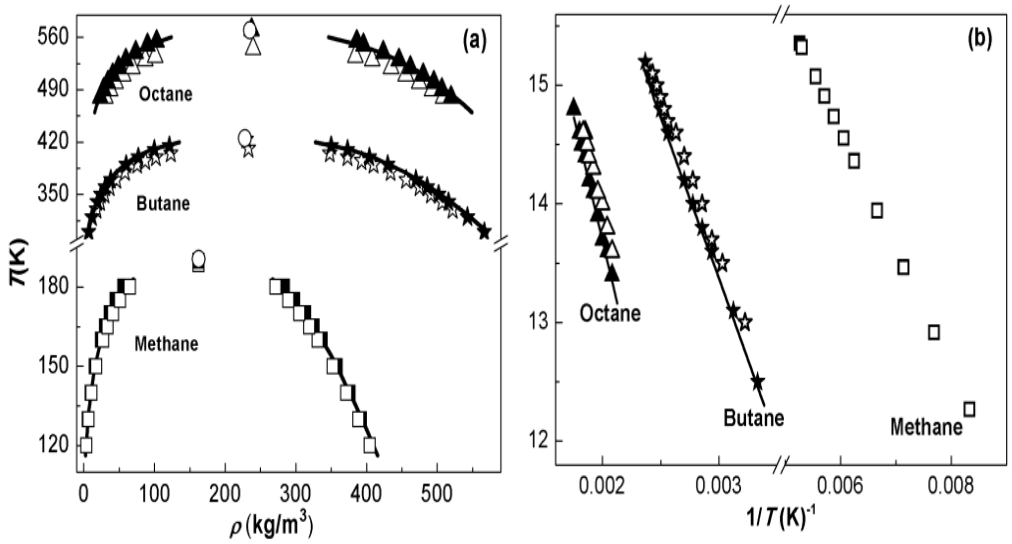

Figure 4.1 (a) Vapor-liquid coexistence envelope and (b) Saturation Pressure of bulk methane-butane and n-octane. Solid lines represent the data of the experiment Filled symbols represents Buckingham potential model (exp-6 model) with full range interaction and open symbols shows the Buckingham potential model with $r_c = 15A^0$[43].

Figure 4.1 (a) shows the bulk phase vapor liquid coexistence curve of methane, n-butane and n-octane based on the Buckingham potential model with cut off, $r_c=15A^0$ and the full range interactions Buckingham potential model along with its experimental data. From this investigation it is observed that the model data of alkanes are in good agreement with the experimental data. Therefore this model is chosen to study the corresponding state behavior of confined alkanes. Moreover, the data obtained with $r_c = 15A^0$ are in reasonably good agreement with the data obtained using full range interaction of the model. Based on this observation we have chosen $r_c = 15A^0$ for all others simulation in this work.

4.2 Effect of interaction range on the corresponding state behavior of bulk n-alkanes.

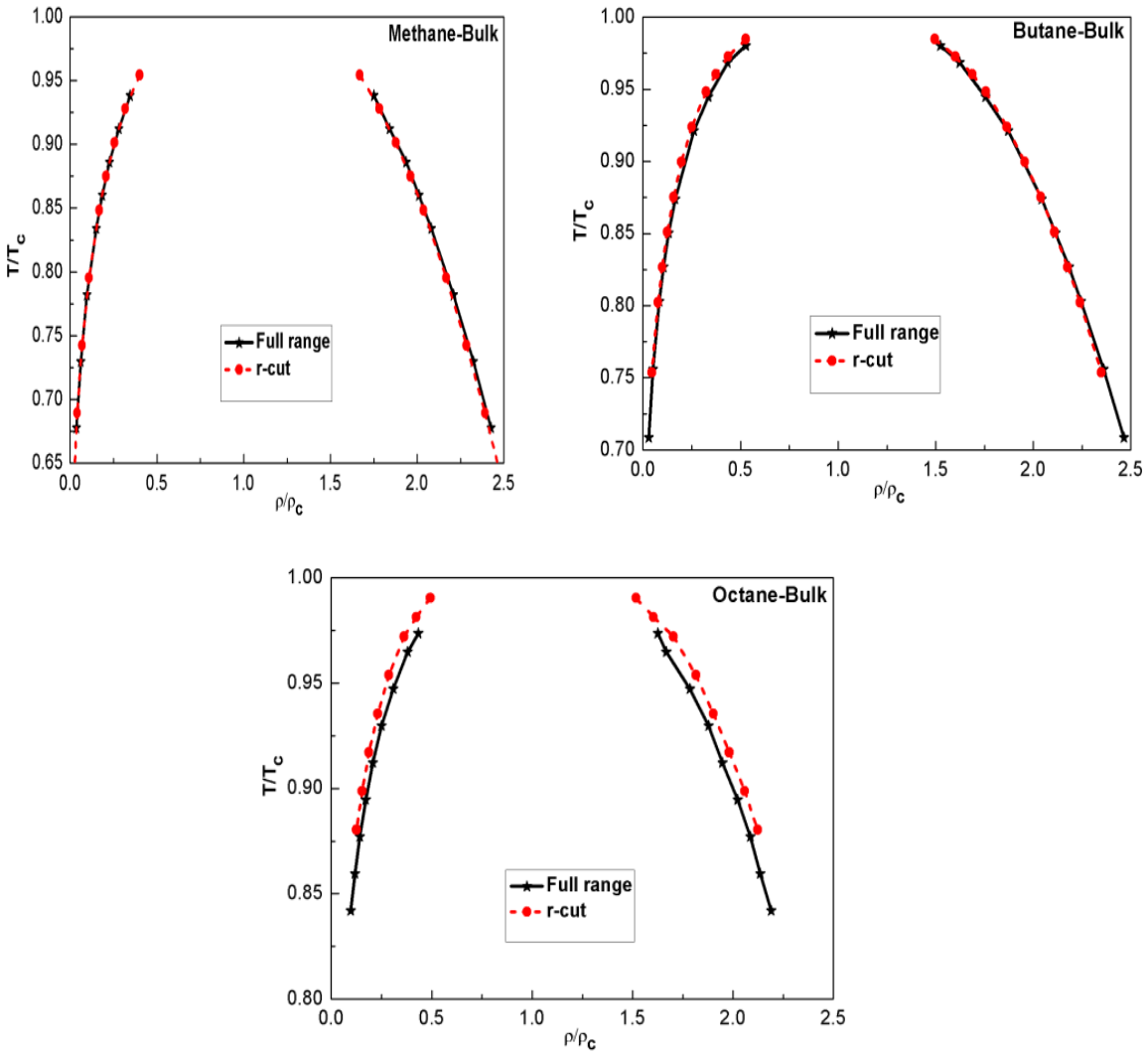

Figure 4.2 Comparison of corresponding state behavior of bulk methane, butane and octane with full range interaction and with r_c= 15A^0.

Figure 4.2 Compares the corresponding state behavior of vapor-liquid phase coexistence of bulk methane, butane and octane with full range interaction and with r_c=15A^0. This investigation reveals that the chosen cut off of Buckingham potential has insignificant effect on the corresponding state behavior of methane and butane .However for n-octane slight deviations in corresponding state behavior is observed with respect to full range interactions. This may be due to the larger size of the octane.

4.3. Corresponding state behavior of bulk and confined methane.

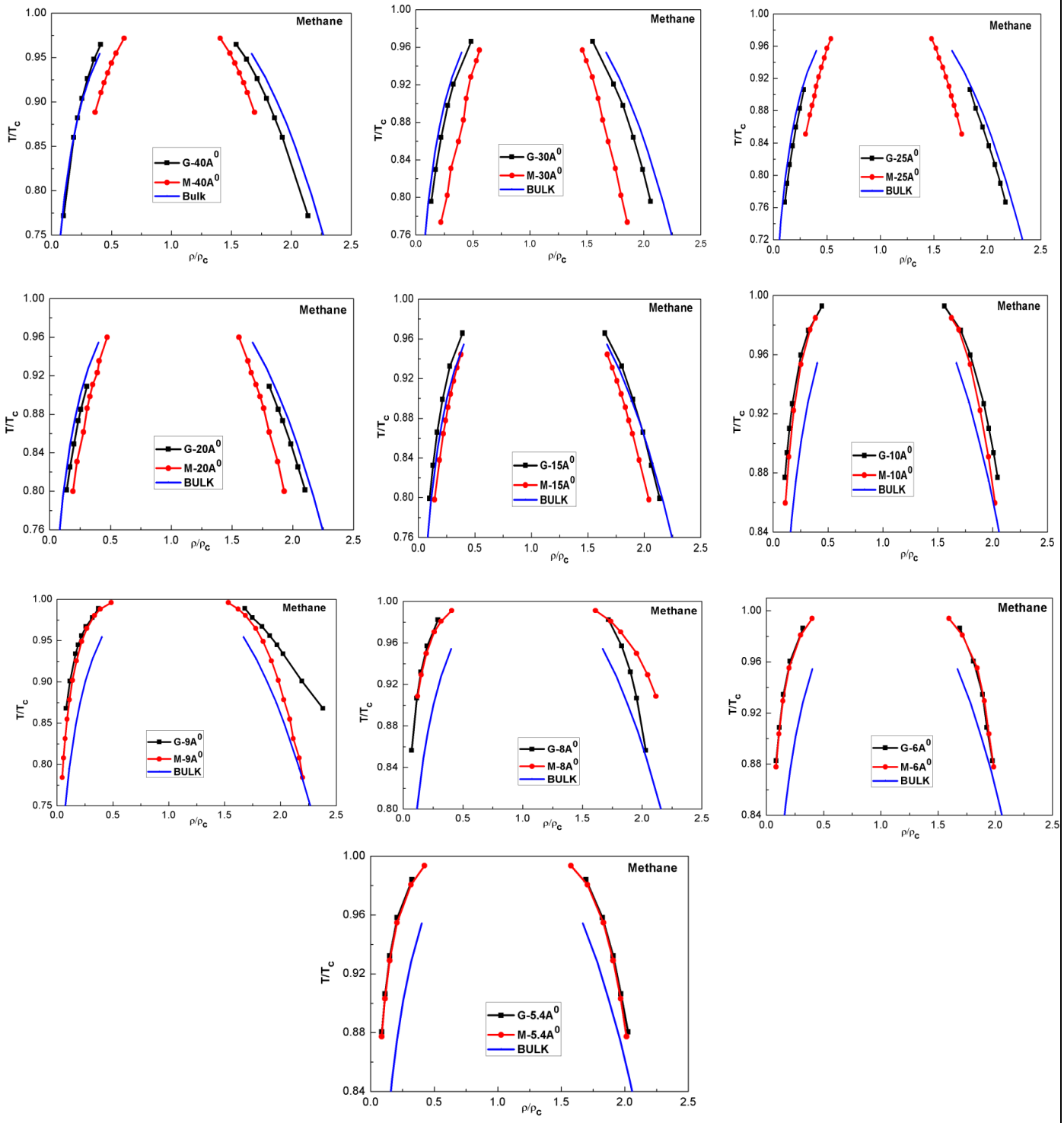

Figure 4.3 Comparison of Corresponding state behavior of bulk and confined methane in graphite and mica slit pores.

Figure 4.3 shows corresponding state behavior of bulk and confined methane in graphite and mica slit pores of various slit width. In this work corresponding state behavior of methane is studied from $40A^0$ to $5.4A^0$.In this investigation from $40A^0$ to $15A^0$ pore width the reduced vapor density of confined methane is comparably larger than that of corresponding bulk vapor density. Moreover, reduced vapor density in mica slit pore is comparably larger than that of graphite slit pore because of stronger surface attraction of methane molecules with mica surfaces. On the other hand, the reduced liquid density in pore width from $40A^0$ to $15A^0$ is comparably larger in graphite slit pore than that in mica slit pore. Moreover, the reduced liquid density of bulk is larger than that of either type of confinement. This investigation further reveals that the corresponding state behavior of confined methane is significantly altered in ultra nano pores. It is observed that in ultra nano pores ($\leq 10A^0$) the reduced vapor density of confined methane is less than the reduced vapor density of corresponding bulk values. On the other hand, the reduced liquid density of confined methane is comparably larger than that of corresponding bulk values. Moreover, from pore width <8 A^0 the corresponding state coexistence envelope of confined fluid fall on one master curve, therefore, revealing insignificant effect of surface chemistry.

4.4 Corresponding state behavior of bulk and confined n-butane.

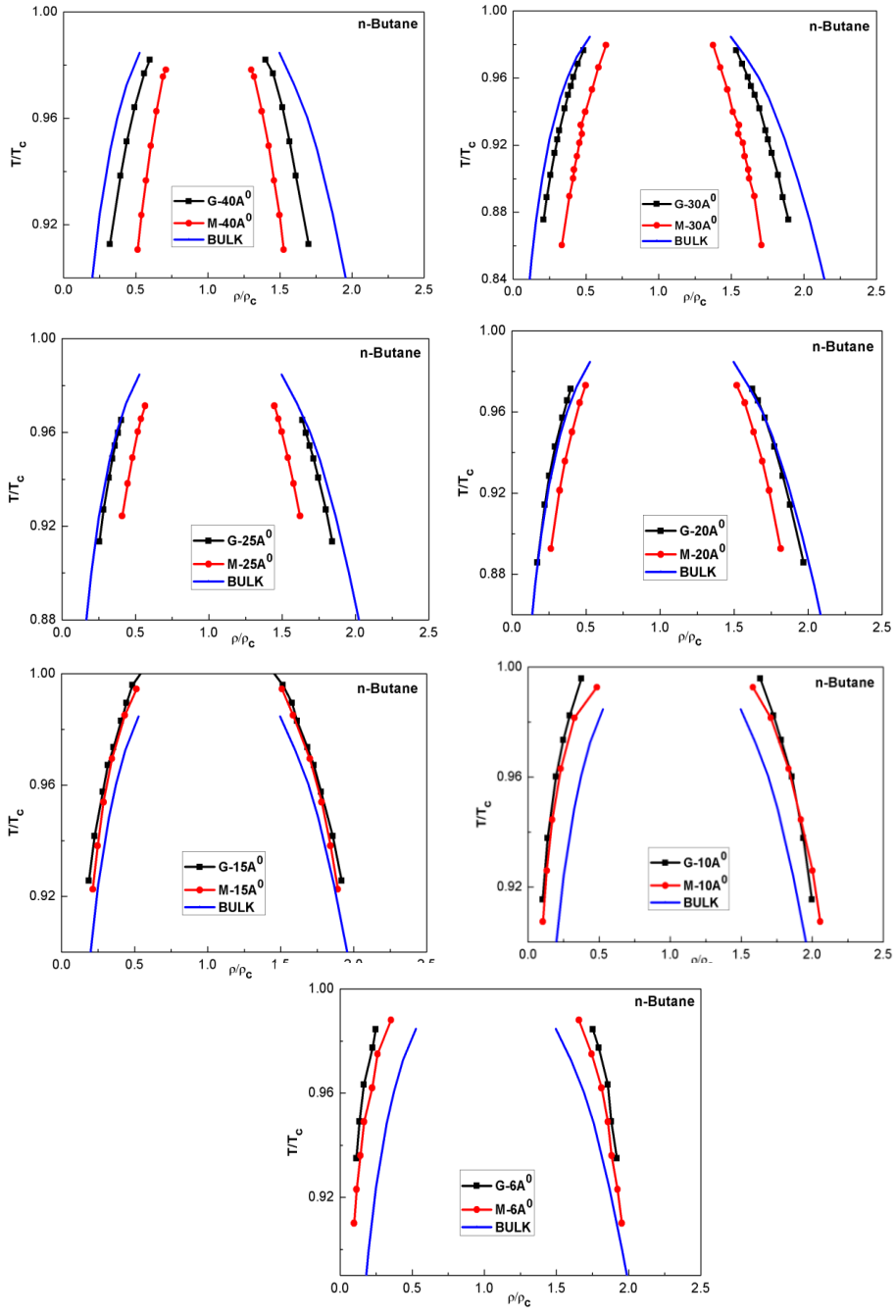

Figure 4.4 Comparison of Corresponding state behavior of bulk and confined butane in graphite and mica slit pores.

Figure 4.4 shows corresponding state behavior of bulk and confined butane in graphite and mica slit pores of various slit width. In this work corresponding state behavior of butane is studied from $40A^0$ to $6A^0$. In this investigation from $40A^0$ to $20A^0$ pore width the reduced vapor density of confined butane is comparably larger than that of corresponding bulk vapor density. On the other hand, the reduced liquid density of bulk is larger than that of either type of confinement. This investigation further reveals that the corresponding state behavior of confined butane is significantly altered in ultra nano pores. It is observed that in ultra nano pores ($\leq 15A^0$) the reduced vapor density of confined butane is less than the reduced vapor density of corresponding bulk values. On the other hand, the reduced liquid density of confined butane is comparably larger than that of corresponding bulk values. Moreover, from pore width < $20A^0$ the corresponding state coexistence envelope of confined butane fall on one master curve, therefore, revealing insignificant effect of surface chemistry.

4.5 Corresponding state behavior of bulk and confined n-octane.

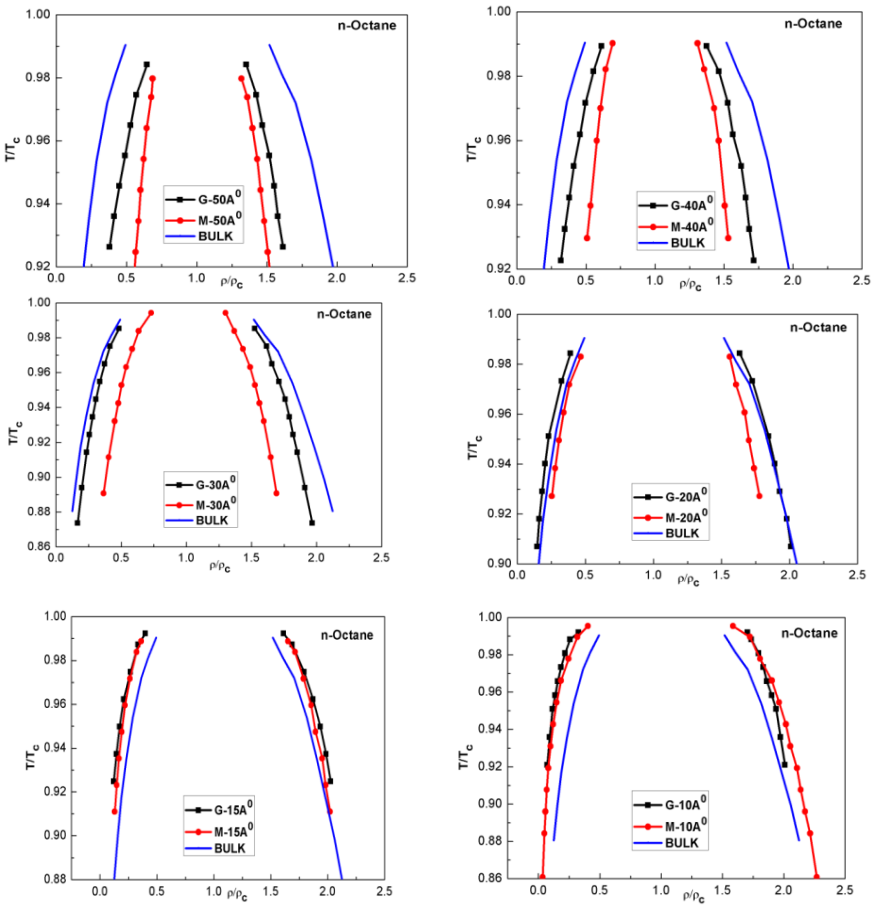

Figure 4.5 Comparison of Corresponding state behavior of bulk and confined octane in graphite and mica slit pores.

Figure 4.5 shows corresponding state behavior of bulk and confined octane in graphite and mica slit pores of various slit width. In this work corresponding state behavior of octane is studied from $40A^0$ to $6A^0$.In this investigation from 50 A^0 to $10A^0$ pore width the reduced vapor density of confined octane is comparably larger than that of corresponding bulk vapor density. On the other hand, the reduced liquid density of bulk is larger than that of either type of confinement. This investigation further reveals that the corresponding state behavior of confined octane is significantly altered in ultra nano pores. It is observed that in ultra nano pores ($\leq 15A^0$) the reduced vapor density of confined octane is less than the reduced vapor density of corresponding bulk values, whereas, the corresponding reduced liquid density is larger for confined octane as compare to bulk octane. Moreover, in these ultra nano pores the corresponding state coexistence envelope of confined octane fall on one master curve, therefore, is revealing insignificant effect of surface chemistry on the corresponding state behavior.

4.6. Comparison of corresponding state behavior of confined alkanes in graphite and mica slit pore.

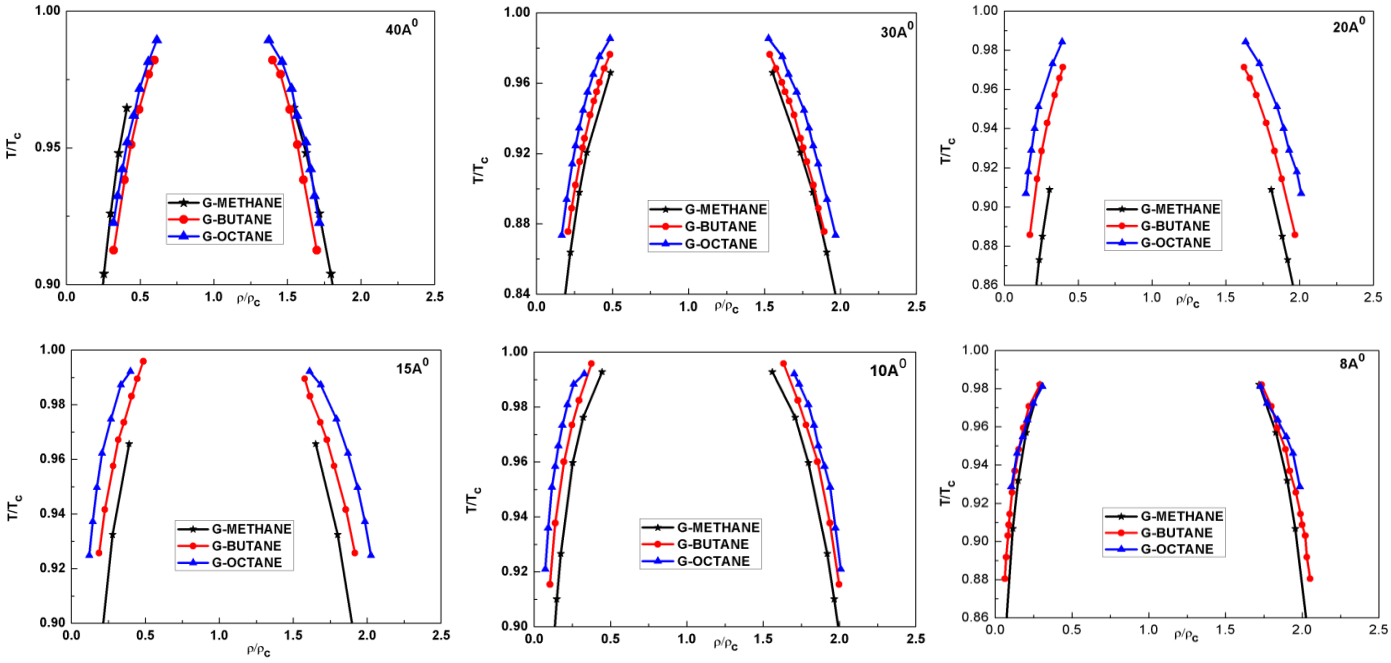

Figure 4.6 (a) Comparison of Corresponding state behavior of confined methane, butane and octane in graphite slit pores.

Figure 4.6 (a) shows corresponding state behavior of confined methane, butane and octane in graphite slit pores of various slit width. In this investigation, it is evident that the effect of molecular shape and size on corresponding state behavior is insignificant in the largest and smallest pore width studied in this work. On the other hand, significant effect of molecular shape and size is observed in the pore width ranging from $30A^0$ to $10A^0$ .In this range ($30A^0$ to $10A^0$) of graphite pore width the reduced vapor density is largest for methane followed by butane and octane respectively. On the other hand, in this range of graphite pore width the reduced liquid is largest for the octane followed by butane and methane. This in turn indicates that the shrinking in corresponding state coexistence envelope is highest for methane than that of butane and octane.

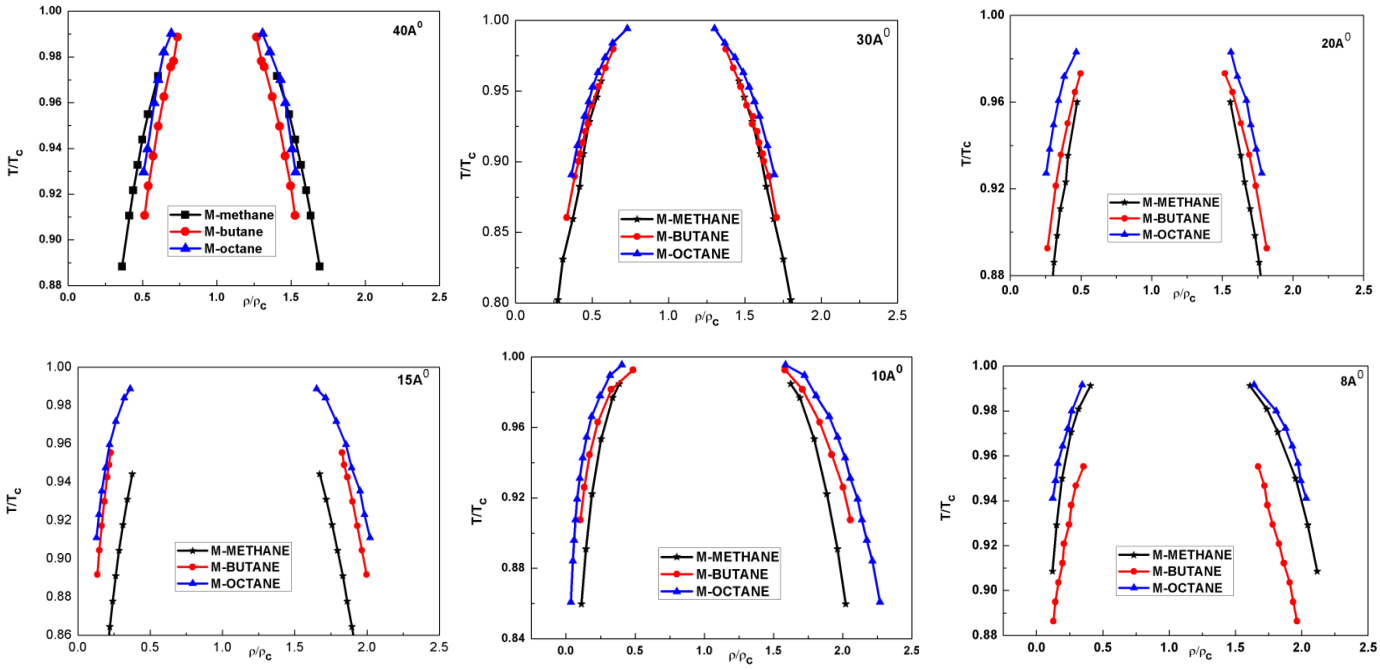

Figure 4.6 (b) Comparison of corresponding state behavior of confined methane, butane and octane in mica slit pores.

Figure 4.6 (b) shows corresponding state behavior of confined methane, butane and octane in mica slit pores of various slit width. In this investigation, we observed similar trend in corresponding state behavior with respect to shape and size of molecules, from $30A^0$ to $10A^0$. In this range ($30A^0$ to $10A^0$) of mica pore width the reduced vapor density is largest for methane followed by butane and octane respectively. On the other hand, in this range of mica pore width the reduced liquid is largest for the octane followed by butane and methane. This in turn indicates that the shrinking in corresponding state coexistence envelope is highest for methane followed by n-butane and n-octane. Moreover, with highest ($40A^0$) and smallest ($8A^0$) pore width the shrinking in corresponding state coexistence envelope is maximum for n-butane. However, methane and octane have shown insignificant change in corresponding state coexistence envelope.

4.7. Comparison of corresponding state behaviour of saturation vapour pressure of bulk and confines alkanes.

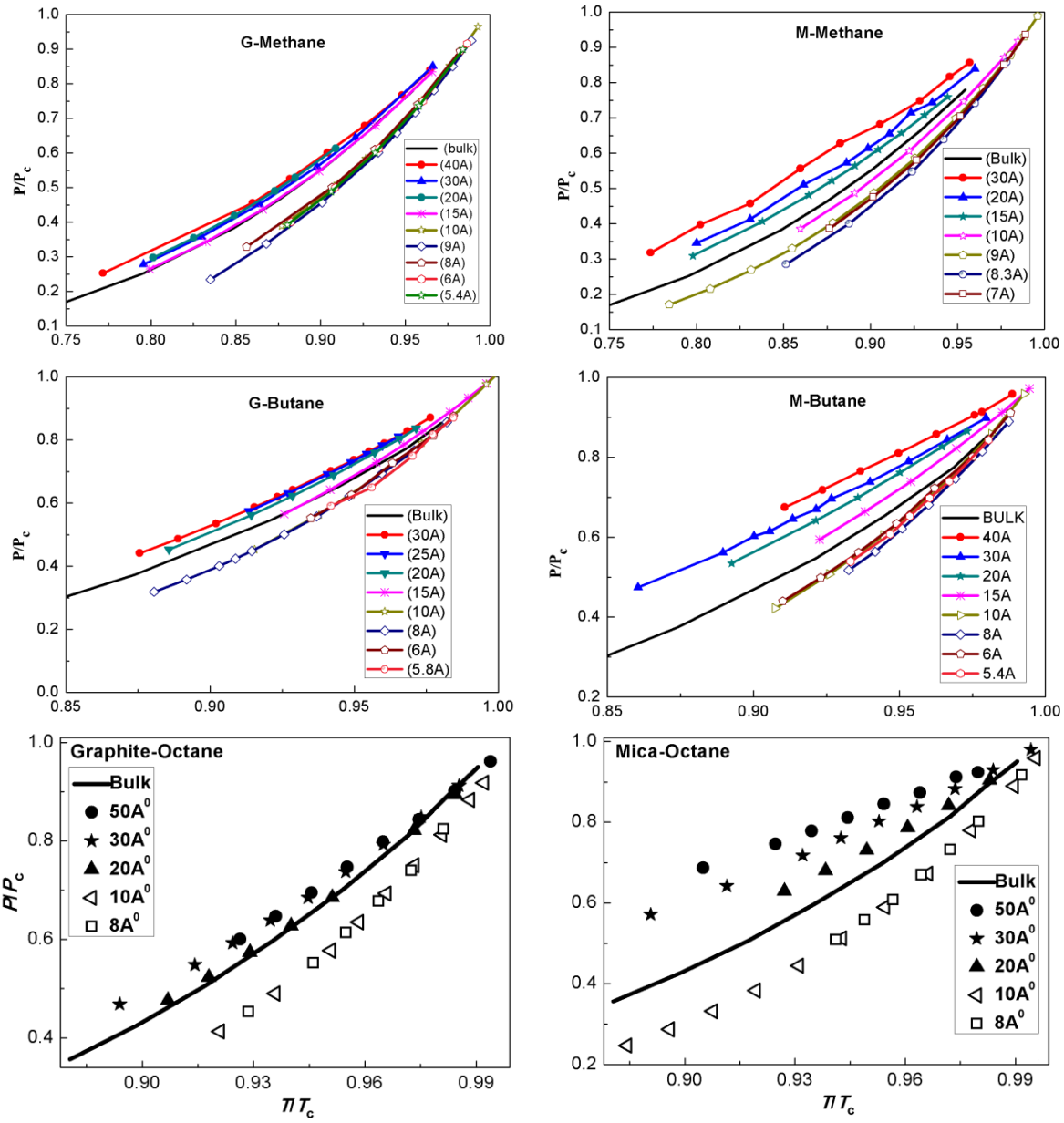

Figure 4.7 Variation of reduced saturation vapour pressures versus reduced temperature of the bulk and confined alkanes in graphite and mica slit pores. Solid lines represent bulk values; filled and open symbols show positive and negative deviations respectively.

Figure 4.7 shows the comparison of saturation vapour pressure of alkanes in confinement with respect to the bulk, in a corresponding state plot. Saturation vapour pressure under either type of confinement (graphite and mica) show positive and negative deviation with respect to bulk value at a given reduced temperature. The saturation vapour pressure at larger slit width is more than that of bulk at a given reduced temperature for methane, n-butane and n-octane confined in graphite and mica slit pores. However, in smaller slit width (as seen from $10A^0$ onwards), irrespective of the studied alkanes, the reduced saturation vapour pressure, is smaller than the corresponding bulk value. A deviation of the reduced saturation vapour pressure from the corresponding bulk value is seen as larger for mica pore for all studied alkanes in this work. This may be due to stronger attraction of mica surfaces with fluid molecules.

CHAPTER-5

CONCLUSIONS

This work illustrates how the pore size and its surface chemistry can alter the vapour-liquid phase equilibrium of a corresponding state of bulk and confined alkanes. In this work, corresponding state behaviour of vapour-liquid coexistence of methane, butane & octane are studied in graphite and mica slit pores of varying pore width & also compared with the corresponding bulk values. In this investigation, under confinement, deviations from corresponding state behaviour is observed with larger pore widths irrespective of fluid under consideration. On the other hand, with smaller pore width insignificant deviations from corresponding behaviour is observed. This investigation also reveals that with mica slit pore shrinking of corresponding state coexistence envelope is comparably more than that of graphite slit pore because of larger surface fluid attraction of mica surface. In this work, we have also compared the saturation vapour pressure in confinement with respect to bulk, in a corresponding state plot. Saturation vapour pressure under either type of confinement (graphite & mica) show positive and negative deviation with respect to the bulk value at a given reduced temperature. A deviation of the reduced saturation vapour pressure from the corresponding bulk value is seen larger for a mica pore as compared to graphite pore because of its stronger attraction with fluid molecules.

CHAPTER- 6

REFERENCES

[1] Chandra, S., Singh, R. K., & SINGH, M. P. (2014). Properties of Materials Confined inNano-pores. *Department of Physics, Banaras Hindu University, Varanasi*, *221*, 005.

[2] Nelson, P. H. (2009). Pore-throat sizes in sandstones, tight sandstones, and shales. *AAPG bulletin*, *93*(3), 329-340.

[3] Singh, S. K., Sinha, A., Deo, G., & Singh, J. K. (2009). Vapor− liquid phase coexistence, critical properties, and surface tension of confined alkanes. *The Journal of Physical Chemistry C*, *113*(17), 7170-7180.

[4] Zhuravlev N. D., Martin M. G., and Siepmann J. I., *Vapor–liquid phase equilibria of triacontane isomers: Deviations from the principle of corresponding states.* Fluid Phase Equilibria, 2002. **202**: p. 307–324.

[5] Prausnitz, J. M., Lichtenthaler, R. N., & de Azevedo, E. G. (1998). *Molecular thermodynamics of fluid-phase equilibria*. Pearson Education.

[6] Singh, J. K., & Kwak, S. K. (2007). Surface tension and vapor-liquid phase coexistence of confined square-well fluid. *The Journal of chemical physics*, *126*(2), 024702.

[7] Gil-Villegas, A., del Río, F., & Benavides, A. L. (1996). Deviations from corresponding-states behavior in the vapor-liquid equilibrium of the square-well fluid. *Fluid Phase Equilibria*, *119*(1-2), 97-112.

[8] McQuarrie, D. A. Statistical Mechanics. 2000, Sausalito.

[9] Guggenheim, E. A. (1966). *Applications of statistical mechanics* (pp. 186-206). Oxford: Clarendon press.

[10] Benavides, A. L., Guevara, Y., & Del Rio, F. (1994). Vapor-liquid equilibrium of a multipolar square-well fluid: I. Effect of multipolar

strengths. *Physica A: Statistical Mechanics and its Applications*, *202*(3-4), 420-437.

[11] del Río, F., Benavides, A. L., & Guevara, Y. (1995). Vapor-liquid equilibrium of a multipolar square-well fluid II. Effect of a variable square-well range. *Physica A: Statistical Mechanics and its Applications*, *215*(1-2), 10-20.

[12] Van Leeuwen, M. E. (1994). Deviation from corresponding-states behaviour for polar fluids. *Molecular Physics*, *82*(2), 383-392.

[13] Vega, C., Lago, S., De Miguel, E., & Rull, L. F. (1992). Liquid-vapor equilibria of linear Kihara molecules. *The Journal of Physical Chemistry*, *96*(18), 7431-7437.

[14] Orea P., Varga S., and Odriozolac G., A heuristic rule for classification of classical fluids:Master curves for Mie, Yukawa and square-well potentials.*Chemical Physics Letters* 2015. **631**: p. 26-29

[15] Singh, J. K., & Errington, J. R. (2006). Calculation of phase coexistence properties and surface tensions of n-alkanes with grand-canonical transition-matrix Monte Carlo simulation and finite-size scaling. *The Journal of Physical Chemistry B*, *110*(3), 1369-1376.

[16] Singh, J. K., Kofke, D. A., & Errington, J. R. (2003). Surface tension and vapor–liquid phase coexistence of the square-well fluid. *The Journal of chemical physics*, *119*(6), 3405-3412.

[17] Orea, P., Duda, Y., Weiss, V. C., Schröer, W., & Alejandre, J. (2004). Liquid–vapor interface of square-well fluids of variable interaction range. *The Journal of chemical physics*, *120*(24), 11754-11764.

[18] López-Rendón, R., Reyes, Y., & Orea, P. (2006). Thermodynamic properties of short-range square well fluid. *The Journal of chemical physics*, *125*(8), 084508.

[19] Jana, S., Singh, J. K., & Kwak, S. K. (2009). Vapor-liquid critical and interfacial properties of square-well fluids in slit pores. *The Journal of chemical physics*, *130*(21), 214707.

[20] Panagiotopoulos, A. Z. (1987). Adsorption and capillary condensation of fluids in cylindrical pores by Monte Carlo simulation in the Gibbs ensemble. *Molecular Physics*, *62*(3), 701-719.

[21] Singh, S. K., Saha, A. K., & Singh, J. K. (2010). Molecular Simulation Study of Vapor− Liquid Critical Properties of a Simple Fluid in Attractive Slit Pores: Crossover from 3D to 2D. *The Journal of Physical Chemistry B*, *114*(12), 4283-4292.

[22] Walton, J. P. R. B., & Quirke, N. P. R. B. (1989). Capillary condensation: a molecular simulation study. *Molecular Simulation*, *2*(4-6), 361-391 *rod mixtures.*Journal of Chem. Phys, 1989. **11**: p. 227-228.

[23] Vanderlick, T. K., Davis, H. T., & Percus, J. K. (1989). The statistical mechanics of inhomogeneous hard rod mixtures. *The Journal of chemical physics*, *91*(11), 7136-7145.

[24] Zarragoicoechea, G. J., & Kuz, V. A. (2004). Critical shift of a confined fluid in a nanopore. *Fluid phase equilibria*, *220*(1), 7-9.*attractive wall-fluid potentials: Critical point shift.* . Physical Review E, 2006. **74**: p. 062601.

[25] Zhang, X., & Wang, W. (2006). Square-well fluids in confined space with discretely attractive wall-fluid potentials: Critical point shift. *Physical Review E*, *74*(6), 062601.

[26] Alharthy, N. S., Nguyen, T., Teklu, T., Kazemi, H., & Graves, R. (2013, September). Multiphase compositional modeling in small-scale pores of unconventional shale reservoirs. In *SPE Annual Technical Conference and Exhibition*. Society of Petroleum Engineers.

[27] Devegowda, D., Sapmanee, K., Civan, F., & Sigal, R. F. (2012, January). Phase behavior of gas condensates in shales due to pore proximity effects: Implications for transport, reserves and well productivity. In *SPE Annual Technical Conference and Exhibition*. Society of Petroleum Engineers.

[28] Zarragoicoechea, G. J., & Kuz, V. A. (2002). van der Waals equation of state for a fluid in a nanopore. *Physical Review E*, *65*(2), 021110..

[29] Hamada, Y., Koga, K., & Tanaka, H. (2007). Phase equilibria and interfacial tension of fluids confined in narrow pores. *The Journal of chemical physics*, *127*(8), 084908.

[30] Devegowda, D., *Phase Behvaiour of Gas Condensates in Shale due to Pore Proximity Effects: Implications for transport , reserves and well productivity*. . 2012.

[31] Teklu, T. W., Alharthy, N., Kazemi, H., Yin, X., Graves, R. M., & AlSumaiti, A. M. (2014). Phase behavior and minimum miscibility pressure in nanopores. *SPE Reservoir Evaluation & Engineering*, *17*(03), 396-403.

[32] Markov, I. V. (2016). *Crystal growth for beginners: fundamentals of nucleation, crystal growth and epitaxy*. World scientific.

[33] Parisi, G., *Statistical Field Theory;*. Vol. 66. 1988, Redwood City,CA: Addison-Wesley Pub.Co.

[34] Berg, B. A., & Neuhaus, T. (1992). Multicanonical ensemble: A new approach to simulate first-order phase transitions. *Physical Review Letters*, *68*(1), 9.

[35] Ukawa, A. (1990). QCD phase transitions at finite temperatures. *Nuclear Physics B-Proceedings Supplements*, *17*, 118-136.

[36] Smit, B., Karaborni, S., & Siepmann, J. I. (1995). Computer simulations of vapor–liquid phase equilibria of n-alkanes. *The Journal of chemical physics*, *102*(5), 2126-2140.

[37] Siepmann, J. I., & Frenkel, D. (1992). Configurational bias Monte Carlo: a new sampling scheme for flexible chains. *Molecular Physics*, *75*(1), 59-70.

[38] Ryckaert, J. P., & Bellemans, A. (1975). Molecular dynamics of liquid n-butane near its boiling point. *Chemical Physics Letters*, *30*(1), 123-125.

[39] Errington, J. R., & Panagiotopoulos, A. Z. (1999). A new intermolecular potential model for the n-alkane homologous series. *The Journal of Physical Chemistry B*, *103*(30), 6314-6322.

[40] van der Ploeg, P., & Berendsen, H. J. C. (1983). Molecular dynamics of a bilayer membrane. *Molecular Physics*, *49*(1), 233-248.

[41] Steele, W. A. (1973). The physical interaction of gases with crystalline solids: I. Gas-solid energies and properties of isolated adsorbed atoms. *Surface Science*, *36*(1), 317-352.

[42] Porcheron, F., Rousseau, B., Fuchs, A. H., & Schoen, M. (1999). Monte Carlo simulations of nanoconfined n-decane films. *Physical Chemistry Chemical Physics*, *1*(17), 4083-4090.

[43] NIST Chemistry web BooK. http:// webbook.nist.gov/chemistry/fluid.

Anjali.docx

ORIGINALITY REPORT

19%	17%	19%	0%
SIMILARITY INDEX	INTERNET SOURCES	PUBLICATIONS	STUDENT PAPERS

PRIMARY SOURCES

1	home.iitk.ac.in Internet Source	16%
2	Singh, Sudhir K., Ankit Sinha, Goutam Deo, and Jayant K. Singh. "Vapor−Liquid Phase Coexistence, Critical Properties, and Surface Tension of Confined Alkanes", The Journal of Physical Chemistry C, 2009. Publication	2%
3	Gil-Villegas, A.. "Deviations from corresponding-states behavior in the vapor-	1%

liquid equilibrium of the square-well fluid",
Fluid Phase Equilibria, 19960515

Publication

EXCLUDE QUOTES	ON	EXCLUDE MATCHES	< 130 WORDS
EXCLUDE BIBLIOGRAPHY	ON		